# Comparative Analysis of 1D MARS-KS and 3D CFD Modeling for Thermal-Hydraulic Characteristics of i-SMR Helical Coil Steam Generator

Je-Hyeong Park [a*], Won-Seok Ryoo [a], Jae-Ho Jeong [a*]
[a]*Mechanical Engineering, Chung-Ang University, Dongjak-gu, Seoul, 06974*
[*]*Corresponding author: jaehojeong@cau.ac.kr*

***Keywords :*** i-SMR, Helical Coil Steam Generator(HCSG), MARS-KS, CFD

## 1. Introduction

In response to global carbon neutrality policies and climate change mitigation efforts, nuclear energy is being reconsidered as a reliable carbon-free energy source. Among advanced nuclear systems, Small Modular Reactors (SMRs) have gained significant attention due to their enhanced safety features and construction flexibility compared to conventional large-scale reactors. In Korea, the development of an innovative Small Modular Reactor (i-SMR) based on indigenous technology is actively underway [1][2].

The i-SMR adopts an integral reactor configuration in which major components are installed within a single reactor pressure vessel. Among these components, the Helical Coil Steam Generator (HCSG) plays a crucial role in removing core heat and transferring thermal energy to the secondary system. The HCSG applied to the i-SMR features large-diameter helical tubes (approximately 3 m in coil diameter), which exceed the geometric range commonly addressed in previous studies on medium- and small-scale helical tubes.

Due to curvature effects, secondary flows are generated inside helical tubes, resulting in asymmetric velocity and temperature distributions across the cross-section. Furthermore, depending on operating conditions, single-phase and two-phase flow regimes may coexist, and the transition between flow regimes can significantly influence thermal-hydraulic performance and system stability. Therefore, a detailed investigation of internal flow characteristics in large-scale HCSG tubes and an evaluation of modeling consistency between system-level codes and high-fidelity CFD simulations are required [3].

In this study, one-dimensional thermal-hydraulic analyses were performed using the MARS-KS system code, and three-dimensional CFD simulations were conducted for the i-SMR HCSG tube. The internal flow and heat transfer characteristics were obtained and compared to assess modeling consistency and applicability limits from a multi-scale analysis perspective.

## 2. Numerical Methodology

### *2.1 MARS-KS System Code Modeling*

To evaluate the system-level thermal-hydraulic characteristics of the i-SMR HCSG, one-dimensional steady-state analyses were performed using the MARS-KS system code. The steam generator was modeled using a nodalization approach consisting of 28 computational cells representing the primary and secondary sides. The initial single-channel configuration was validated and subsequently extended to a two-channel model to improve physical representation.

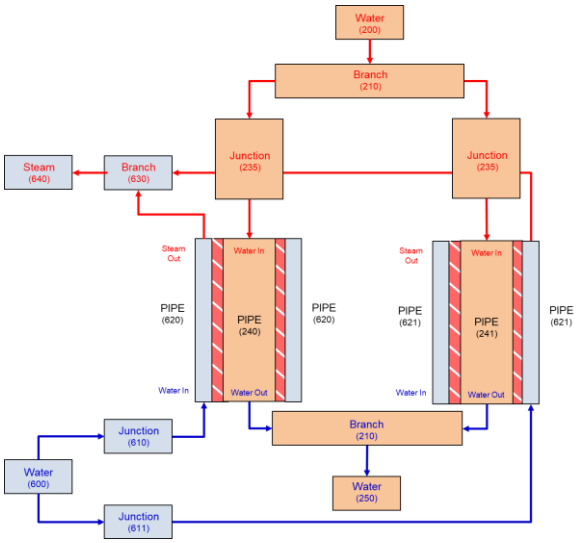


Fig. 1. MARS-KS nodalization scheme for the i-SMR steam generator

MARS-KS employs a two-fluid model based on the conservation equations of mass, momentum, and energy for each phase [4][5]. The general form of the governing equations can be expressed as:

Conservation of Mass:

$$\frac{\partial}{\partial t}(\alpha_k \rho_k) + \nabla \cdot (\alpha_k \rho_k \boldsymbol{U}_k) = \Gamma_k \qquad (1)$$

Conservation of Momentum:

$$\frac{\partial}{\partial t}(\alpha_k \rho_k \boldsymbol{U}_k) + \nabla \cdot (\alpha_k \rho_k \boldsymbol{U}_k \boldsymbol{U}_k) = \alpha_k \rho_k \boldsymbol{g} - \alpha_k \nabla \rho + \nabla \cdot [\alpha_k (\boldsymbol{\tau}_k + \boldsymbol{T}_k^T)] + \boldsymbol{M}_k^\tau + \boldsymbol{M} \qquad (2)$$

Conservation of Energy:

$$\frac{\partial}{\partial t}(\alpha_k \rho_k h_k) + \nabla \cdot (\alpha_k \rho_k h_k \boldsymbol{U_k}) = -\nabla \cdot [\alpha_k (\boldsymbol{q}_k + \boldsymbol{q}_k^T)] + \Gamma_k h_k^i + q_{Ik}^{"} + \alpha_k \frac{\partial P}{\partial t} \quad (3)$$

where $\alpha_k$, $\rho_k$, $U_k$ and $h_k$ are the volume fraction, density, velocity, and specific enthalpy of phase $k$, respectively; bold symbols denote vectors/tensors.

Flow regime transitions were determined based on void fraction criteria, enabling identification of bubbly, slug, annular, and mist flow regions along the axial direction. The predicted outlet temperature and pressure drop were compared with design values prior to CFD comparison.

### *2.2 i-SMR HCSG CFD Modeling*

Three-dimensional CFD simulations were conducted to investigate detailed flow and heat transfer characteristics within the helical coil tube. Although the reference i-SMR HCSG comprises 5,128 helical tubes, the present analysis focused on a single-tube domain assumed to be representative of the overall system. To evaluate curvature effects, three geometries were considered: a non-helical straight tube, a one-pitch-scale helical tube, and a full-scale helical tube corresponding to the i-SMR design.

Structured meshes were generated to accurately capture axial development and curvature-induced secondary flow structures, as illustrated in Fig. 2. The final full-scale configuration consisted of approximately 4.8 million computational cells, determined based on mesh sensitivity considerations. The shear stress transport (SST) k–ω turbulence model was adopted to resolve near-wall behavior and secondary flow formation.

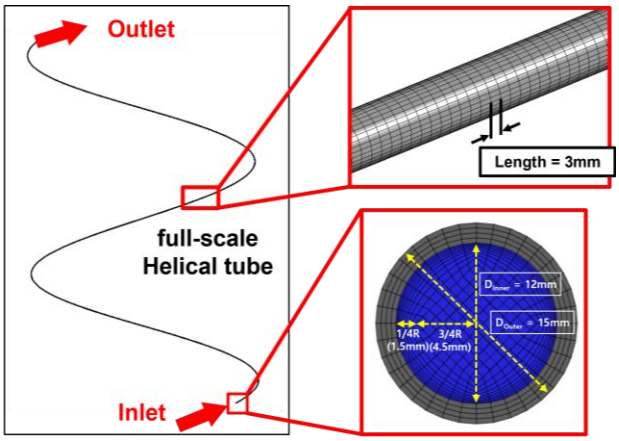


Fig. 2 i-SMR HCSG full-scale computational grid system

The CFD domain was limited to the tube-side flow region. On the tube side, the inlet mass flow rate, inlet temperature, inlet pressure, and outlet pressure were specified based on the design condition. The primary side was not explicitly resolved in the CFD model; instead, the steady-state MARS-KS primary-side results were used to determine the heat duty, which was converted into a uniform wall heat flux and imposed on the outer tube wall. Although the present CFD analysis was limited to a preliminary single-phase simulation, the imposed wall heat flux included the latent heat contribution to maintain energy consistency with the MARS-KS system-level analysis.

Table I: CFD Boundary Conditions and Primary-Side Reference Conditions

| Parameter | Value |
|---|---|
| Primary-side mass flow rate [kg/s] | 2381.6 |
| Primary-side inlet temperature [°C] | 320.22 |
| Primary-side inlet pressure [MPa] | 15.06 |
| Tube-side Mass flow rate [kg/s] | 281.8 (Re ≈ 53,139) |
| Tube-side Inlet temperature [°C] | 243.81 |
| Tube-side Outlet pressure [MPa] | 5.3 |

## 3. Results

The MARS-KS steady-state analysis demonstrated clear axial flow regime transitions along the tube. In the single-channel model, the bubbly-to-slug transition occurred around the 9th cell, while the slug-to-annular transition was identified near the 16th cell based on the void fraction criterion. In the two-channel configuration, the bubbly-to-slug transition shifted upstream to around the 5th–6th cell, while the annular transition occurred near the 17th–18th cell. Near the outlet region, mist and horizontally stratified flow regimes were predicted.

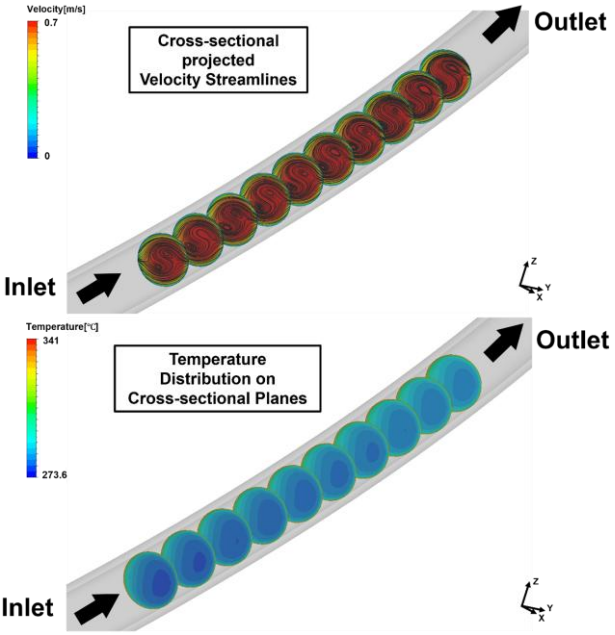


Fig. 3. Flow and Temperature Distributions in a Full-Scale Helical Tube

The temperature differences predicted by MARS-KS showed good agreement with the design values. The primary-side ΔT deviation was approximately 3.1%, and the tube-side ΔT deviation was within 5.9%, confirming the reliability of the system-level modeling.

The CFD simulations captured curvature-induced secondary flow structures in the helical configuration, which were absent in the straight tube case. Representative cross-sectional velocity streamlines and

temperature distributions for the full-scale helical tube are shown in Fig. 3. Due to centrifugal effects, higher velocity magnitudes were observed along the outer curvature, resulting in asymmetric temperature distributions across the cross-section.

Direct comparison of outlet temperatures revealed that the single-phase CFD prediction (≈565 °C) significantly exceeded the MARS-KS result (≈297 °C). This discrepancy arises from the inability of single-phase CFD modeling to physically represent latent heat effects under boiling conditions. When latent heat effects were evaluated separately through an energy-based estimation, the predicted outlet temperature approached the MARS-KS result, reducing the deviation to within approximately 1–6%. A quantitative comparison of the overall tube-side pressure drops for the helical tube also showed a noticeable discrepancy between MARS-KS and the preliminary single-phase CFD result (0.22 MPa vs. 0.07 MPa). This suggests that the present CFD model, which is limited to single-phase tube-side flow with an imposed wall heat flux, cannot fully reproduce the boiling-induced density variation and two-phase pressure-loss mechanisms represented in MARS-KS.

These findings indicate that the discrepancies originate from modeling assumptions rather than numerical inconsistency and highlight the necessity of multiphase CFD analysis for rigorous validation of boiling heat transfer and pressure-drop behavior in large-diameter helical steam generator tubes.

## REFERENCES

[1] International Atomic Energy Agency, Climate Change and Nuclear Power 2022, 2022.
[2] S. G. Lim, et al., Design Characteristics of Nuclear Steam Supply System and Passive Safety System for Innovative Small Modular Reactor (i-SMR), Nuclear Engineering and Technology, 2025, p. 103697.
[3] Y. Ko and H. K. Cho, Improvements of First and Total Dry-out Models for the Helical Coiled SGs, Transactions of the Korean Nuclear Society Spring Meeting, Jeju, Korea, May 22–23, 2025.
[4] Y. M. Kwon, et al., SSC-K User's Manual, Korea Atomic Energy Research Institute, Technical Report No. KAERI/TR-1619/2000, 2000.
[5] Korea Atomic Energy Research Institute, MARS Code Manual, Volume I: Code Structure, System Models, and Solution Methods, KAERI/TR-2812/2004, December 2009.